Saturn hexagon - a telltale of quantum gravity

Farid Abrari

1400 Woodeden Dr, Mississauga, Ont, L5H 2T9, Canada

farid.abrari@gmail.com

July 24, 2021

Abstract

The quantized model of Newtonian gravity indicates that the quantum effects of gravity become apparent when particles of *sufficiently small mass* are in the orbit of a gravitating body of mass. In particular, the stable orbital path of particles in such conditions are shown to be polygons. The stable circular path of classical mechanics emerges when the side counts of these polygons increase to infinity, as the quantum effects of gravity vanish due to the excessive mass of the orbiting particles. In this article, it is hypothesized that the particle mass in Saturn's North Pole jet stream is such that the quantum effects of gravity have become apparent. The hexagonal shape of Saturn's jet stream is therefore used to constrain the mass of its cloud particles to 7.4E-20 (kg). This in turn constrains the dimensions of ammonia ice crystals in the clouds to less than 100 nanometers. This theory also indicates that polygons of different side counts are also feasible at different latitudes, should the local particle mass permit the quantum effects of gravity to become visible. This aspect of the theory is also consistent with the presence of faint but still visible *edges* of some polygons at lower latitudes.

Keywords — Quantum Gravity, Saturn Hexagon, Saturn Polygons, combined SR-QM theory

1   Introduction

Saturn's North Pole hexagonal jet stream [1] was first discovered in the images taken by the Voyager 1 and 2 flyby missions in early 1980's and it has been observed repeatedly since then for nearly 40 years. All observations, including those of Cassini mission in 2006-2007 indicate that the hexagon is not a seasonal phenomenon but rather a long term feature of Saturn's North Pole cloud system. The observations throughout the North Pole region also indicate that the cloud systems are not shallow dynamical features but rather deeply penetrate into the Saturnian atmosphere, indicative of little vertical shear in depths of several hundred kilometers [2]. While the formation mechanism of the hexagon is not satisfactorily understood, a few hypothesises have been suggested to describe the phenomenon behind the formation of the highly unusual shape of the jet stream, including vertically trapped Rossby wave oscillations [3], barotropic [4] or baroclinic instabilities in the flow [5]. Recently, a supersymmetric operator originally developed for the quantized 2D electromagnetic fields was used to model Saturn's hexagon at the macroscopic scales [6]. In this paper, an alternative explanation is proposed which is based on the quantum gravity. While the theory does not deal with the complex gas dynamics of the hexagon cloud system, it nonetheless provides a foundation for the quantum gravitational aspects of the phenomenon which can be subsequently implemented in a representative numerical model of the weather system.

2   Background

In [8], it was shown that the local acceleration of a particle with rest mass m falling freely in the gravitational field of a much larger body of mass M is given as:

$$\frac{GM}{R_{\dot{n}}^2} = \dot{n}c\sqrt{\frac{\bar{m}}{m}} \qquad \dot{n} = 1, 2, ... \tag{1}$$

where $\dot{n}$ is understood to be the *quantum rate index*; a positive integer with the unit of $\sec^{-1}$, R is the distance between the masses, G is the gravitational constant and c is the speed of light. The physical interpretation of the scaling reference mass $\bar{m} = h/Ac$ with the *estimated* rest mass of $3.2E - 45$ (kg) was also introduced in [7, 8]. Furthermore, it was shown that for particles of *minuscule* mass, the 3D gravitational field surrounding a large body of mass M appears to be in the form of a series of *spherical shells of constant gravity* which are increasingly tight-packed as altitude drops. As shown in Fig 1, for a given pair of masses m and M, the spacing (or width) of such spherical shells (or rings in 2D cross-section) is quantized as follows [8]:

$$x_{\dot{n}} = \sqrt[4]{\frac{m}{\bar{m}}} \left(\sqrt{\frac{GM}{\dot{n} \cdot c}} - \sqrt{\frac{GM}{(\dot{n}+1) \cdot c}} \right) \qquad \dot{n} = 1, 2, ... \tag{2}$$

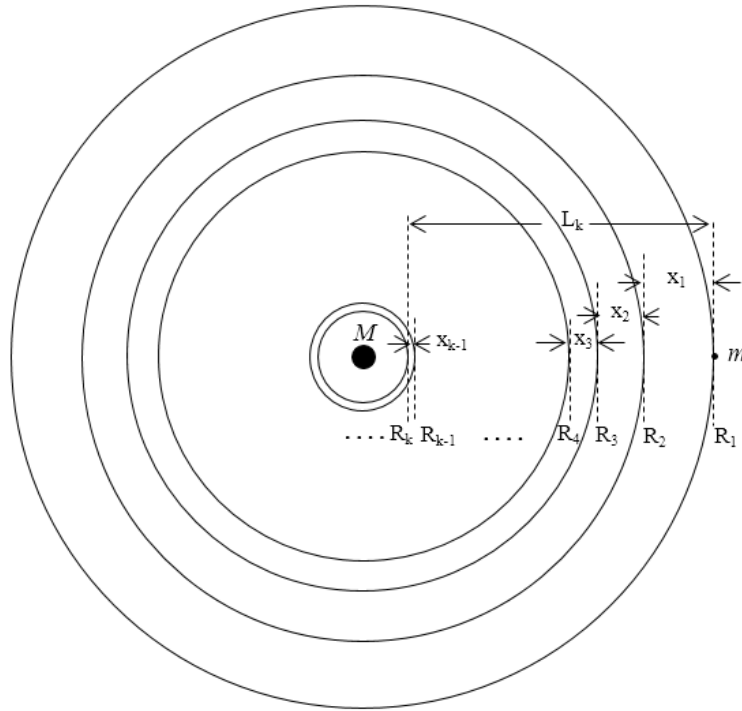Due to the smooth and continuous nature of the Newtonian gravity, the width of such spherical

Figure 1: The rings of constant gravity progressively narrow down in width as altitude drops

shells of constant gravity is obviously zero in the classical Newtonian gravity. In the latter, as a consequence, the only possible trajectory on which the gravitational force acting on an orbiting particle could remain constant is that of a *perfect circle*. As discussed earlier, in the quantum model of gravity, in contrast, there exists a spatial interval $x_{\dot{n}}$ within which the force of gravity is invariant; and as a consequence, the particle trajectory could deviate from the perfect circular path as long as the particle remains within the ring of constant gravity. As a result, *the orbital path of minuscule particles where quantum effects of gravity are apparent is always an polygon rather than a circle* [9]. It is clear that the extent of the trajectory deviations from the circular path of the classical

mechanics is a function of the width of the ring of constant gravity. In other words, as shown in Fig 2, the wider the ring of constant gravity, the more significant the effect of quantum gravity; and hence, the higher the deviations from the perfect circular path are expected to be. The side-count
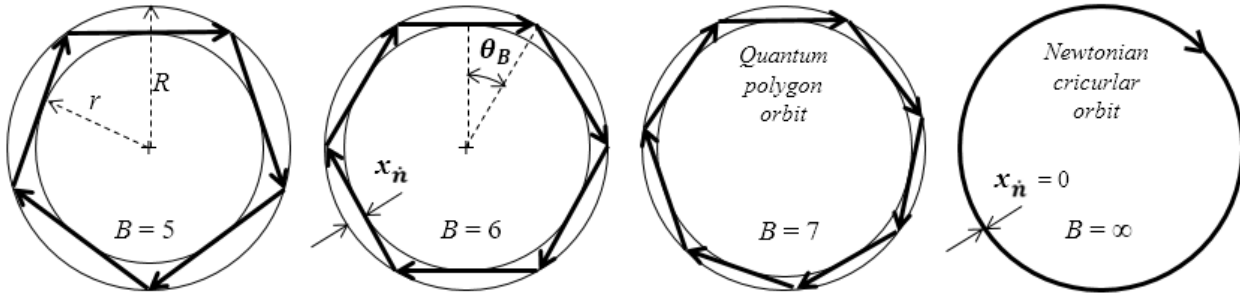

Figure 2: Quantum polygon orbit within rings of constant gravity v.s. classic circular orbit

parameter B of a *regular polygon* and the ratio of the radii of the *inscribed* to the *circumscribed* circles are related as follows:

$$\frac{r}{R} = \cos(\theta_B) \tag{3}$$

where $\theta_B = \pi/B$ is the complement of half of the interior angle of a polygon of side count B. In Fig 2, moving from left to right, we note that as the width of the ring of constant gravity reduces, i.e. as the effect of quantum gravity diminishes, the polygonal orbital path of quantum gravity gets closer and closer to the classical Newtonian circular path. At the limit, where the quantum effects of gravity completely vanish, and subsequently the width of constant gravity ring drops to zero, the side-count parameter $B \to \infty$ and the polygonal orbital path of quantum gravity reduces to the classical circular orbit. As shown in Fig 3, as the side count of a regular polygon increases, the
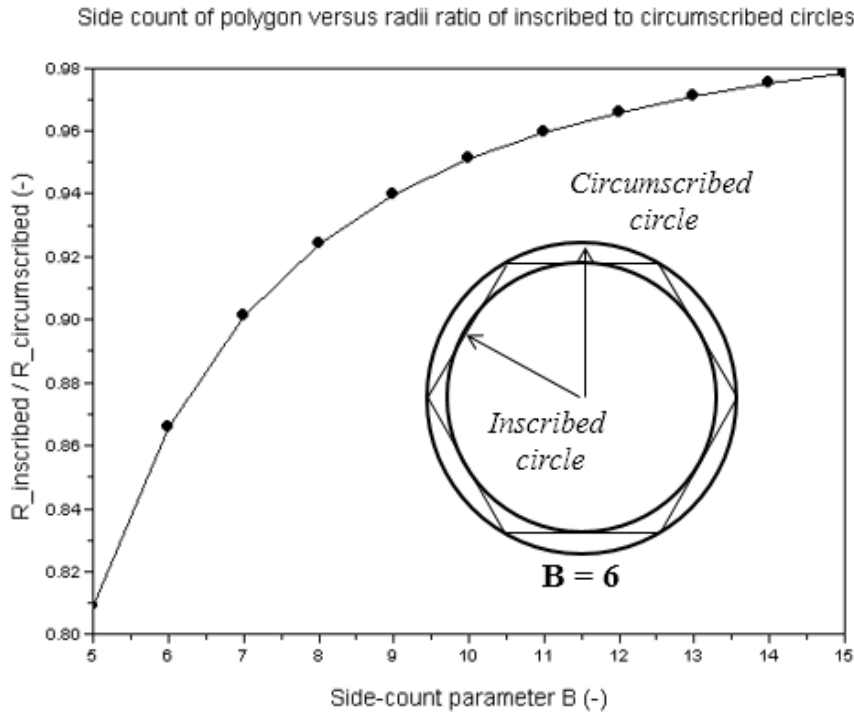

Figure 3: Gap of constant gravity reduces to zero as $B \to \infty$ (Newtonian circular orbit)

ratio of radii of the inscribed to circumscribed circles approaches to one. For a hexagon the ratio is around 0.866. Before concluding this section let's remark here that at certain rings of constant

3

gravity the orbital path of the individual particles change from being an *open polygon*, as shown in Fig 4a, into a closed *regular polygon*, as shown in Fig 4b. In other words, the orbital path of the individual particles in such ring widths change from being *precessional* to fully *repeatable* and non-precessional ones. In general, the polygon path of the particles in such rings, while now repeatable, would still be *out-of-phase* relative to each other. This, as shown in Fig 5a, may seem to prevent the particles in those rings to self-organize into a common streamline. However, in such conditions, the individual particles would repeatedly intersect each other at certain points along the orbit, hence, mutually influence each other's path into an *average* one as shown in Fig 5b. In time, this will then make the path of individual particles to become *in-phase* with each other and generate a collective pattern in their motion; a possibility that does not exist in the precessional orbital paths.
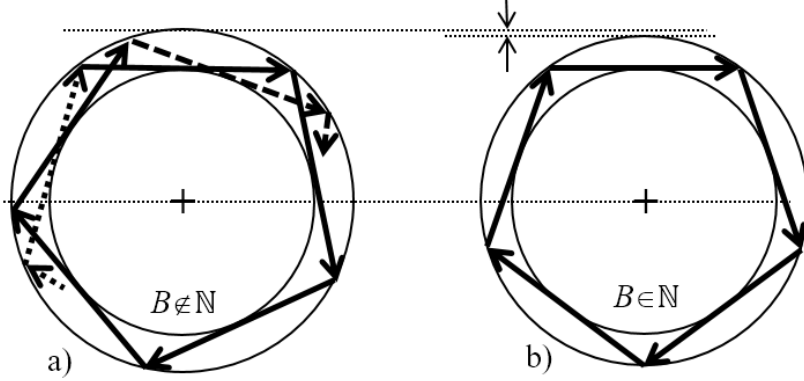

Figure 4: a) An open precessional orbit b) Closed regular polygon of a non-precessional orbit
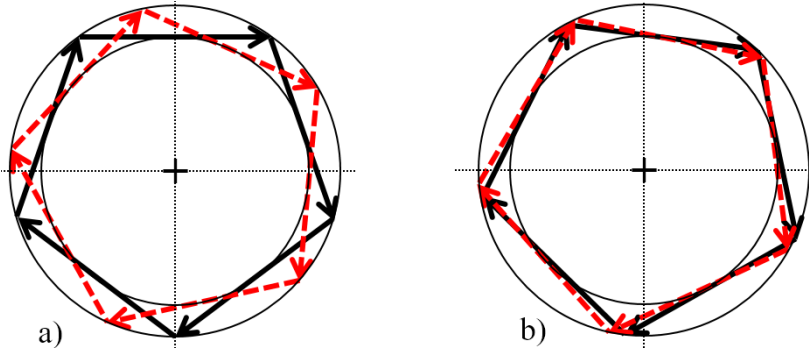

Figure 5: a) Out of phase trajectories of a pair of particles b) Average in-phase trajectories

3   Particle mass constrain of Saturn hexagon

Fig 6a shows a meridian cut through the North Pole of Saturn in which a spherical shell from the planet's atmosphere is seen as a ring of constant width inside the outermost periphery of the planet. In Fig 6b, a top view of the North Pole is shown in which a planar cut is passing through a hexagonal jet stream at 78 degrees latitude [10]. The atmospheric spherical shell has, therefore, such a width that it encompasses the hexagonal jet stream at that latitude. The hexagonal trajectory on the plane of cut is therefore tangent to the boundaries of the spherical shell at radii R_6 and r_6 at 12 points in total (i.e. 6 points on the inscribed circle and 6 points on the circumscribed circle). Applying the quantum theory of gravity to this situation, we hypothesize that *the particle mass m in the hexagon jet stream is such that its acceleration quanta matches with the centripetal*

acceleration difference across the distance $R_6 - r_6$. Therefore:

$$\frac{v_o^2}{r_6} - \frac{v_o^2}{R_6} = c\sqrt{\frac{\bar{m}}{m}} \tag{4}$$

where v_o is the observed velocity of the particles in the jet stream. From Eqn 4, we then have the
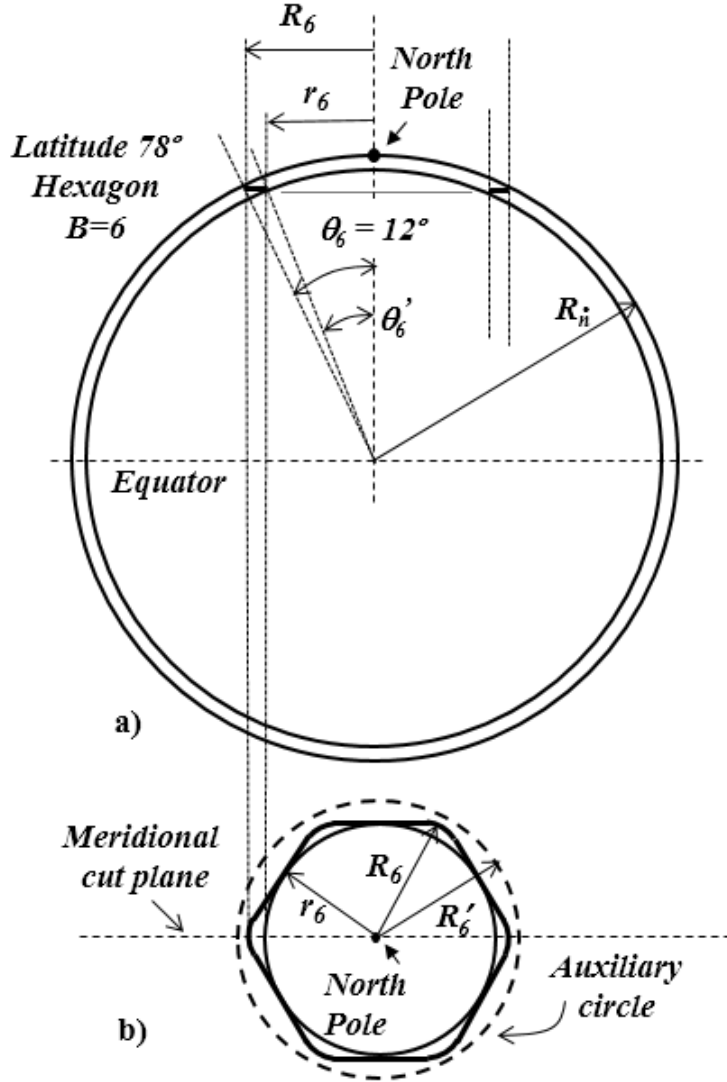

Figure 6: a) Meridional section of the spherical shell encompassing hexagon b) top view

following equation for the cloud particles' mass m:

$$m = \frac{c^2}{v_o^4} \left(\frac{R_6 r_6}{R_6 - r_6}\right)^2 \bar{m} \tag{5}$$

In general, for a polygonal trajectory of side count B, the radii R_B and r_B are given as follows [9]:

$$R_B = \frac{r_B^2 + 0.25\beta^2}{\beta} \tag{6}$$

$$r_B = \frac{0.5\beta}{\cos(\pi/B)}$$

where β is the defining parameter of the vertex parabola and the angle $\theta_B = \pi/B$, as discussed earlier, is the *complement of half of the interior angle* of the polygon. Solving for the ratio r_B/R_B,

5

we then have:

$$\frac{r_B}{R_B} = \frac{2}{\cos(\pi/B) + csc(\pi/B)} \tag{7}$$

Using this highly simplified closed form equation, the ratio corresponding to a hexagonal trajectory (i.e. side count $B = 6$) is found to be $r_6/R_6 = 0.989$. However, observational data from Cassini's photos of the hexagon jet streams constrains the ratio to $r_6/R_6 \approx 0.93$. Therefore, instead of the ratio 0.989 of Eqn 7, the observed ratio 0.93 is used to determine the radii R_6 and r_6. Hence, using Eqn 5, the mass of particles in the hexagonal jet stream (HJS) at 78 degrees latitude is then estimated to be $m_{HJS} = 7.4E - 20$ (kg). In this estimate, the reference particle mass $\bar{m} = 3.2E - 45$ (kg) [8] and jet stream velocity $v_o = 100$ (m/sec) [1] are used. In comparison, the mass of an ammonia molecule is about $m_{ammonia} = 2.828E - 26$ (kg). Accordingly, the hexagon jet stream particle is therefore found to be about $2.6E6$ times more massive than a single ammonia molecule. By taking the size of an $NH3$ molecule as 0.326 (nm), this constrains the size of ammonia ice crystals in Saturn's hexagon clouds to about 45 (nm). Sensitivity of the ammonia ice crystal size to the reference particle mass $\bar{m}$ and the latitudinal angle of a hexagonal trajectory is shown in Fig 7. According to these results from the theory, the dimensions of ammonia ice crystals in Saturn's hexagon may be less than 100 nanometers. If the size of cloud particles were known from Cassini's final plunge into the planet, the data could be used inversely to estimate the mass of the reference particle $\bar{m}$. From Fig 7, it is expected that the mass of particles in the clouds closer to the North Pole be lower than those of lower latitudes.

Before concluding this section, note that with Saturn mass $M = 5.683E26$ (kg), radius $R_{\dot{n}} = $
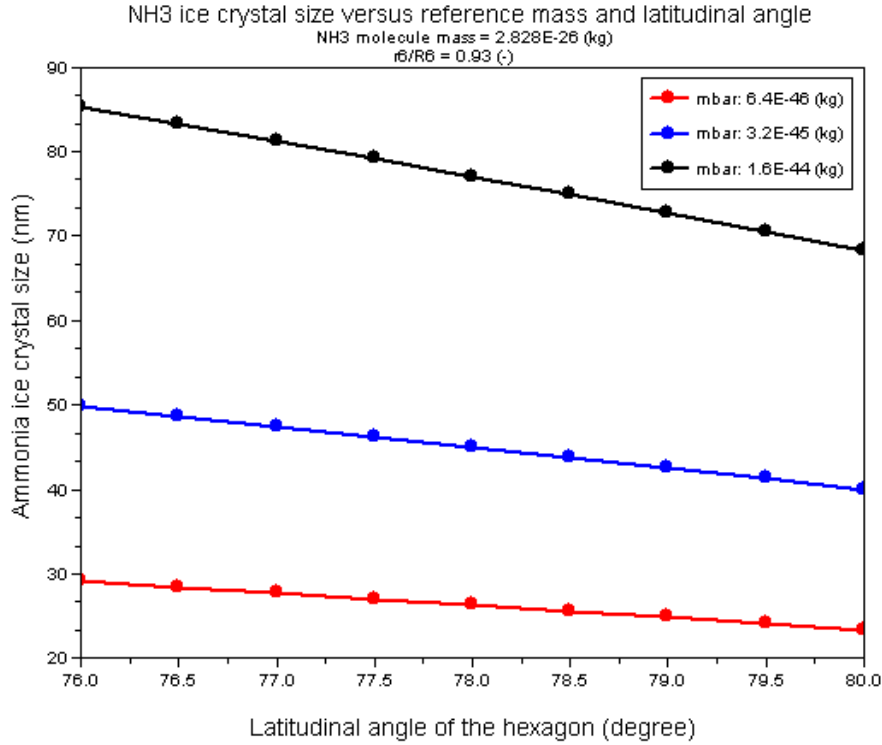

Figure 7: Sensitivity of cloud particle mass on hexagon latitudinal position and $\bar{m}$

$R_{saturn} = 58,232$ (km) and the particle mass $m = 7.4E - 20$ (kg), the quantum rate index from Eqn 1 at the outermost skin of the atmosphere is $\dot{n} = 179,922$ sec^{-1}. Therefore, the height of the *gravitational* quantum ring wherein the planet's gravity at the top of the atmosphere remains invariant is given by $R_{\dot{n}} - R_{\dot{n}+1} = 161.8$ (m). The *action distance* [8] of Saturn in relation to the particle is $R_1/R_{saturn} = 424.1$. Finally, the *attractable mass limit* [8] of Saturn is $m_s = (\frac{c}{g_s})^2 \bar{m} = 2.299E - 30$ (kg); therefore, cloud particles are about $3.24E10$ times more massive than the lightest mass that Saturn could gravitationally bind to.

4   Other polygons of Saturn

It is now evident that depending on the particle mass within a cloud system in a given latitude, the ring of constant centripetal acceleration $R_B - r_B$ would have a different width. The latter, would then permit a polygon of different side count than $B = 6$ to be generated within the ring. For example, in Fig 8 it appears that per one side of the hexagon band, there are roughly 2.5 sides of some polygon at a lower latitude [13]. Therefore, it appears that at the time of this Cassini photo, or similar ones [14, 15, 16], the local particle mass in the clouds were such that a pentadecagon (a 15-sided polygon) could be permitted within the ring of constant centripetal acceleration.
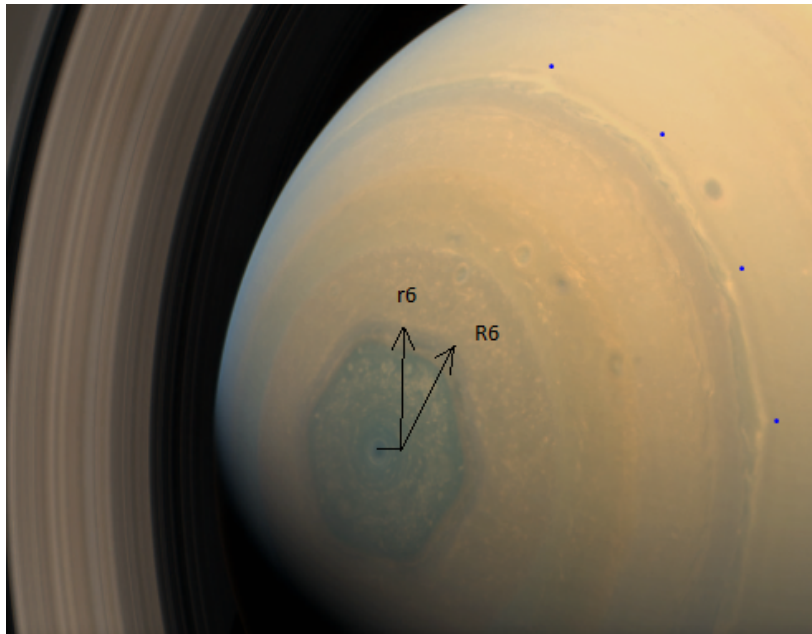

Figure 8: A few edges of a seemingly pentadecagon is visible at a lower latitude [13]

5   Conclusion

The combined theory of Special Relativity-Quantum Mechanics (SR-QM) was previously used to quantize the smooth Newtonian model of gravity. The quantized model of gravity, was shown to generate polygonal trajectories; if the orbiting particles have sufficiently small mass for the quantum effects of gravity to be revealed. In this article, the quantum theory of gravity was applied to Saturn's hexagon in order to constrain the mass/size of the cloud particles. It was found that a stable hexagon trajectory could be established if ammonia ice crystals in the cloud system are less than 100 nanometers in size. The theory also indicates that, depending on the local cloud particles' mass, polygons of a different side-count than 6 are feasible at different latitudes. This aspect of the theory is consistent with the presence of faint but still visible *edges* of polygons at lower latitudes.

References

[1] D. A. Godfrey, 'A hexagonal feature around Saturn's North Pole', Icarus 76, 335-356, 1988

[2] K. H. Baines, et. al. 'Saturn's north polar cyclone and hexagon at depth revealed by Cassini/VIMS', Planetary and Space Science, V57, 1671-1681, 2009

[3] M. Allison, et. al. 'A wave dynamical interpretation of Saturn's polar hexagon', Science 247, 1061-1063, 1990

[4] A. C. B. Aguiar, et. al. 'A laboratory model of Saturn's north polar hexagon', Icarus 206, 755-763, 2010

[5] Y. Lian, A. P. Showman, 'Deep jets on gas-giant planets', Icarus 194, 597-615, 2008

[6] S. Manzetti, A. Trunev, 'Modelling the North-Pole hexagon of Saturn using a supersymmetric wave-equation', Technical Report, DOI: 10.13140/RG.2.2.25077.52963, Aug 2019

[7] F. Abrari, 'Combined theory of Special Relativity and Quantum Mechanics', https://viXra.org/abs/2106.0167

[8] F. Abrari, 'Quantum description of Newtonian gravity', https://viXra.org/abs/2107.0004

[9] F. Abrari, 'Polygonal orbital path of quantum gravity', https://viXra.org/abs/2107.0012

[10] A. Sanchez-Avega, et. al. 'The long term steady motion of Saturn's hexagon and the stability of its enclosed jet stream under seasonal changes', Goephys. Res. Lett., 41, 1425-1431, 2014

[11] L. N. Fletcher, et. al. 'A hexagon in Saturn's northern stratosphere surrounding the emerging summertime polar vortex', Nature communications, DOI: 10.1038/s41467-018-06017-3, 2018

[12] European Space Agency, 'Saturn's famous hexagon may tower above the clouds', ScienceDaily, www.sciencedaily.com/releases/2018/09/180905155444.htm , 5 September 2018

[13] https://ar.pinterest.com/pin/491666484303828350/

[14] https://solarsystem.nasa.gov/news/13037/a-vexing-hexagon/

[15] https://earthsky.org/space/haze-saturn-hexagon-cassini-hubble/

[16] https://astronomy.com/news/2018/09/saturns-hexagon-could-be-an-enormous-tower/